Pinning action of correlated disorder against equilibrium properties of $HgBa_2Ca_2Cu_3O_x$

J. R. Thompson,[1,2] J. G. Ossandon,[3] L. Krusin-Elbaum,[4] D. K. Christen,[1] H. J. Kim,[2,*] K. J. Song,[2,†] K. D. Sorge,[2,‡] and J. L. Ullmann[5]

[1]*Oak Ridge National Laboratory, Oak Ridge, Tennessee 37831-6061, USA*
[2]*Department of Physics, University of Tennessee, Knoxville, Tennessee 37996-1200, USA*
[3]*Department of Engineering Sciences, University of Talca, Curico, Chile*
[4]*IBM Watson Research Center, Yorktown, New York 10598, USA*
[5]*Los Alamos National Laboratory, Los Alamos, New Mexico 87545, USA*

(Received 7 September 2003; published 24 March 2004)

We report significant alteration of the equilibrium properties of the superconductor $HgBa_2Ca_2Cu_3O_x$ when correlated disorder in the form of randomly oriented columnar tracks is introduced via induced fission of Hg nuclei. From studies of the equilibrium magnetization M_{eq} and the persistent current density over a wide range of temperatures, applied magnetic fields, and track densities up to a ''matching field'' of 3.4 T, we observe that the addition of more columnar tracks acting as pinning centers is progressively offset by reductions in the magnitude of M_{eq}. Invoking anisotropy-induced ''refocusing'' of the random track array and incorporating vortex-defect interactions, we find that this corresponds to increase in the London penetration depth λ; this reduces the vortex line energy and consequently reduces the pinning effectiveness of the tracks.

DOI: 10.1103/PhysRevB.69.104520 PACS number(s): 74.25.Qt, 74.25.Op, 74.25.Ha, 74.25.Sv

I. INTRODUCTION

Much has been done over the past decade or so to understand the interaction of superconducting vortices in high-T_c cuprates with correlated disorder, which generally gives strong vortex pinning. Most widely studied have been columnar defects, which typically are formed by irradiation with energetic heavy ions; such particles are highly ionizing and create tracks of amorphous material along their path.[1] Many morphologies have been investigated, ranging from the familiar parallel tracks to inclined defects, crossed arrays with ''designer splay,'' etc. Early theoretical insights and ideas came from Nelson and Vinokur[2] and Hwa *et al.*[3] Numerous experimental studies have shown that such defects are supremely efficient in localizing vortices to their vicinity. This is manifest through strong enhancements of critical (J_c) and persistent current densities in some regions of the phase space. It is also clear that outside these confined regions the localization effects are lessened, in part by the complex vortex (variable range hopping) dynamics[4] which interferes and competes with pinning.

Vortex pinning by proton-generated fission defects was first demonstrated in Bi-cuprate materials[5,6] and can be generally applied in cuprate superconductors that contain a sufficient density of heavy nuclei.[7] The method was devised to circumvent a problem of generating columnar defects (CD's) by heavy-ion irradiation, namely, their limited range, typically a few tens of micrometers. Krusin-Elbaum *et al.*[5] demonstrated an indirect formation of columnar defects by irradiation with deeply penetrating 0.8 GeV protons. An incident proton is absorbed by a heavy nucleus (Hg in the present case) in the material, excites it, and induces it to fission into two particles with similar mass. The recoiling fission fragments, each having $\sim$100 MeV energy, form randomly oriented CD's deep within the superconductor. In a different approach, Weinstein and co-workers created CD's by doping a superconductor with ^{235}U, which is induced to fission by irradiation with thermal neutrons.[8] High-T_c materials containing randomly oriented CD's exhibit a variety of interesting physical phenomena, e.g., a temperature-independent quantum tunneling of vortices in Bi-2212 materials.[9] In studies of Hg-cuprates containing one, two, and three adjacent CuO layers, it was shown[10] that sufficiently high superconductive anisotropy can lead to a rescaling of the splayed landscape of random CD's. As a consequence, the pinning array and the applied field are ''refocused'' toward the crystalline *c* axis, even in polycrystalline materials. Later we use this feature for interpreting the present studies.

In addition to providing vortex pinning sites, correlated disorder doubtlessly also affects the equilibrium superconducting properties, e.g., the characteristic length scales such as λ and ξ. What is little known, however, is how this alters the pinning landscape; for example, an increase in λ will reduce the vortex line energy and hence the pinning force will be reduced.

In this work, we examine the equilibrium magnetization M_{eq} in the mixed state of the anisotropic cuprate $HgBa_2Ca_2Cu_3O_x$, both in its virgin state and when containing randomly splayed columnar defects installed by fission. For virgin Hg-1223, M_{eq} can be scaled following a recent formulation.[11,12] With the addition of splayed CD's, the magnitude of M_{eq} decreases significantly, especially at low fields. In addition, the defects generate a pronounced deviation from the ''standard'' London field dependence, giving an anomalous ''S'' shape to plots of M_{eq} versus $\ln(H)$. By using the concept that sufficiently large anisotropy rescales the random track collection into an equivalent parallel defect array,[10] we apply—in addition to a conventional London description—the vortex-defect interaction model by Wahl *et al.*,[13] which considers a Poisson distribution of parallel tracks. We show that the S shape of M_{eq} is accounted for by the magnetic coupling between defects and vortices. The London penetration depth λ significantly and progressively increases, in accordance with the Wahl-Buzdin description.

This effect counteracts the nominally positive influence of increasing the defect density B_Φ and it plays a major role in determining the level of B_Φ that maximizes the current density J_c.

II. EXPERIMENTAL ASPECTS

Samples for study were bulk polycrystalline $HgBa_2Ca_2Cu_3O_x$ materials (Hg-1223) containing sets of three adjacent oxygen-copper layers. As described in detail by Paranthaman,[14] the starting materials were synthesized in a single step, solid-state reaction using stoichiometric quantities of HgO, BaO, CaO, and CuO. The resulting porous material (with mechanical density ~70% of the x-ray density) was annealed in 1 atm of oxygen at 300 °C, which elevated the superconductive transition temperature T_c to 133–134 K. Small pieces, typically 30 mg mass and ~1 mm thickness, were all cut from the same pellet. The samples were irradiated at room temperature in air with 0.8 GeV protons at the Los Alamos National Laboratory. Proton fluences ϕ_p were 0, 1.0, 3.2, 10, 19, and 35×10^{16} protons/cm^2, as determined from the activation of Al dosimetry foils. The resulting density of fission events is $N/V = \phi_p \sigma_f n_{\mathrm{Hg}}$. Here n_{Hg} is the number density of Hg nuclei and $\sigma_f \simeq 80$ mb is the cross section for inducing a prompt fission of Hg nuclei. Each fission produces one CD, so N/V is the volume density of defects, also. One can convert this into an approximate area density of CD's by multiplying by the track length ~8 μm, and the area density can be reexpressed in units of a matching field B_Φ by multiplying by the flux quantum Φ_0. Resulting values for the defect density are $B_\Phi = 0$, 0.1, 0.3, 1.0, 1.9, and 3.4 T, respectively, for the proton fluences used. The fission process is random in direction, giving randomly oriented CD's. Transmission electron microscopy studies of both Bi-2212 and Hg cuprates[15] have demonstrated the presence of randomly oriented columnar defects in these high-T_c materials.

The superconductive properties of the virgin and processed samples were investigated magnetically. A superconducting quantum interference device based magnetometer (model quantum design MPMS-7), equipped with a high homogeneity 7 T superconductive magnet, was used for studies in the temperature range 5–295 K, in applied fields to 6.5 T. The superconductive transition temperatures T_c were measured in an applied field of 4 Oe (0.4 mT) in zero-field-cooling and field-cooling (FC) modes. The resulting values for the onset temperature T_c are 133, 134, 132.3, 132, 131, and 129.3 K, respectively. Values for the Meissner (FC) fraction $-4\pi M/H$ lie in the range of 40–50 %, except at the highest fluence where the fractional flux expulsion was 29%.

The isothermal magnetization M was measured as a function of applied magnetic field. Below T_c and below the irreversibility line, the magnetization was hysteretic due to the presence of intragrain persistent currents. From the magnetic irreversibility $\Delta M = [M(H\downarrow) - M(H\uparrow)]$, the persistent current density J was obtained using the Bean critical state relation $J \propto \Delta M/r$, where $r \approx 4$ μm is the mean grain radius. Measurements of the background magnetization in the normal state above T_c were used to correct the data in the superconducting state; the background signal was largest (~0.4 G) at the maximum field of 6 T, giving an uncertainty of $\leqslant$0.05–0.1 G in the equilibrium magnetization M_{eq}. Above the irreversibility line where $\Delta M = 0$, this process yields M_{eq} directly. Near the irreversibility line where ΔM is small, we obtain M_{eq} from the (background-corrected) average magnetization $[M(H\downarrow) + M(H\uparrow)]/2$, as illustrated in the following section. This averaging procedure, which follows from the Bean critical state model, is least reliable when the magnetic hysteresis ΔM is large, i.e., in lower magnetic fields. For the irradiated Hg-1223 materials, we estimate the associated uncertainty in M_{eq} to be $\leqslant$0.2–0.3 G at the lowest fields used, 0.15 T, and less in larger fields.

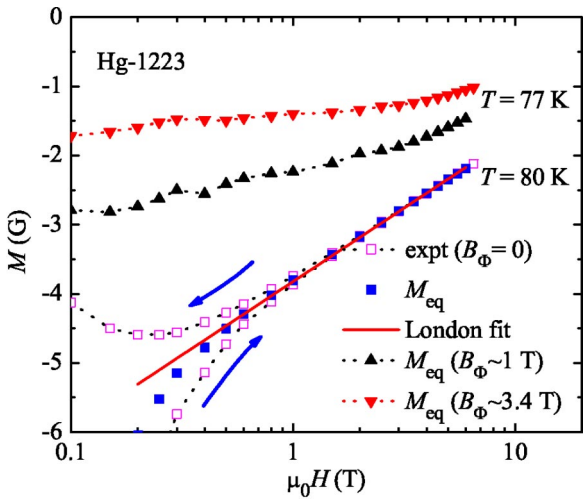

FIG. 1. (Color online) The magnetization of virgin Hg-1223 at 80 K vs applied magnetic field (log scale). Open squares show the measured M in increasing and decreasing field history, while closed squares show the average $M \approx M_{eq}$. The solid line is a fit to the conventional London ln(H) dependence. Data for Hg-1223 containing randomly oriented columnar defects are included for comparison.

III. EXPERIMENTAL RESULTS

A. Equilibrium Properties of Virgin Hg-1223

We begin by considering the equilibrium magnetization in the mixed state. Figure 1 illustrates the method used to obtain M_{eq} by plotting the background-corrected experimental magnetization for the virgin material (open squares) versus applied magnetic field $\mu_0 H$ on a logarithmic scale. As described above, the closed symbols show the average M, which provides a very good approximation to M_{eq} when the hysteresis is small. The solid line is a fit to conventional London theory, which provides that M_{eq} is directly proportional to $(1/\lambda_{ab}^2)\ln(\beta B_{c2}/H)$, where λ_{ab} is the in-plane London penetration depth, $\beta \approx 1.4$ is a constant[16] of order unity, and B_{c2} is the upper critical field.[17] More explicitly, one has with $H \| c$ axis of a uniaxial superconductor that

$$M_{eq} = -(\Phi_0/32\pi^2\lambda_{ab}^2)\ln(\beta H_{c2}/H). \quad (1)$$

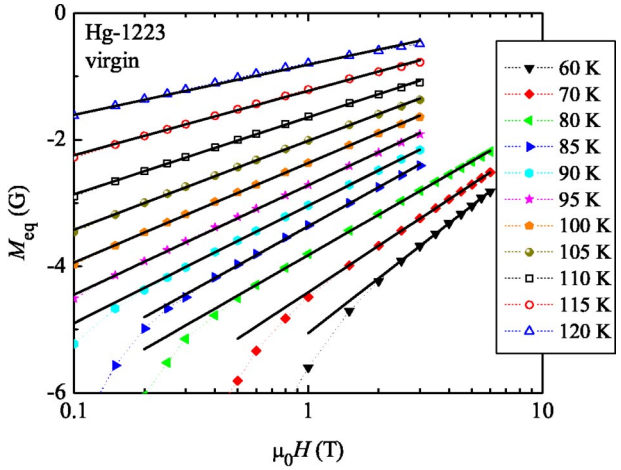

FIG. 2. (Color online) The equilibrium magnetization $M_{eq}(H,T)$ plotted vs ln(H) for unirradiated Hg-1223 at the temperatures shown. Lines are fits to conventional London theory.

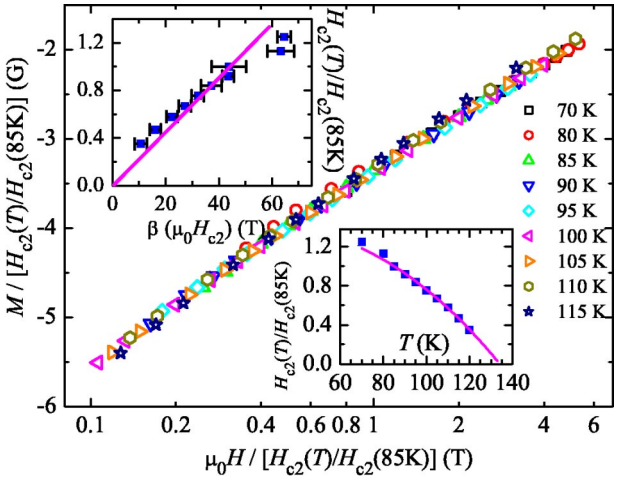

FIG. 3. (Color online) Scaling of the magnetization and applied field by the (relative) upper critical field h_{c2} for virgin Hg-1223. Lower inset shows scaling field h_{c2} vs T, fitted to Eq. (5) (solid line). Upper inset compares values for h_{c2} with results for βH_{c2} from London analysis in Fig. 2.

If H is oriented at angle θ with respect to the c axis, the resulting response can be obtained from the anisotropy function[18]

$$\varepsilon(\theta)=[\cos^2(\theta)+(1/\gamma^2)\sin^2(\theta)]^{1/2}, \tag{2}$$

where $\gamma=(m_c/m_{ab})^{1/2}$ is the mass anisotropy ratio. For a randomly oriented polycrystalline material, the angularly averaged equilibrium magnetization is

$$\langle M_{eq}\rangle=-(\Phi_0/32\pi^2\lambda_{ab}^2)[(1/2)\ln(\beta H_{c2}/H)+(1/4)] \tag{3}$$

in the limit that γ is large.

The straight line fit in Fig. 1 shows that the London ln(H) logarithmic variation describes the field dependence well. Also shown for immediate qualitative comparison are data for M_{eq} of irradiated samples (at 77 K) with defect densities $B_\Phi \approx 1.0$ and 3.4 T.

Results for M_{eq} in the virgin Hg-1223 material at other temperatures are presented in Fig. 2. One sees from the linear regression lines that the London field dependence is followed over a wide range of fields and temperatures. Deviations from linearity occur at low fields when H approaches H_{c1} where simple London theory is not valid, and at low temperatures where the materials are sufficiently hysteretic that the averaging procedure illustrated in Fig. 1 is not valid. From Eq. (3) and the slopes of the curves in Fig. 2, we obtain values for the London penetration depth $\lambda_{ab}(T)$ in the virgin material. These results will be compared and contrasted with values deduced for the irradiated Hg-1223. In addition, the intercepts provide a measure of the upper critical field $e^{1/2}\beta B_{c2}(T)$, where $e \approx 2.718\ldots$ is the natural logarithm base. We now compare these results with those from a scaling analysis.

Recently, Landau and Ott[11] demonstrated a useful scaling methodology based on Ginzburg-Landau theory. This has been applied to both single crystal and aligned particle arrays[11] and more recently to randomly oriented, polycrystalline superconductors.[12] If one assumes that the Ginzburg-Landau parameter $\kappa=\lambda/\xi$ is independent of temperature, then $M_{eq}(H,T)$ is a unique function of $H/H_{c2}(T)$. Consequently, it follows that the equilibrium magnetizations in field H at temperature T and (arbitrary) reference temperature T_0 are related as follows:

$$M(H,T_0)=M(h_{c2}H,T)/h_{c2}, \tag{4}$$

where $h_{c2}=H_{c2}(T)/H_{c2}(T_0)$. To apply this scaling relationship, we chose $T_0=85$ K and manually varied h_{c2} to superposition the data for each temperature. [While a term of the form $c_0(T)H$ was included in the original analysis[11,12] to account for additional contributions to M, we took a minimalist approach of having h_{c2} as the sole parameter.] The results are shown in Fig. 3, which plots M/h_{c2} versus H/h_{c2} for a wide range of temperatures. Given the simplicity of the approach, the scaling is quite good. The results for $h_{c2}(T)$, shown in the lower inset, are well behaved. Following Landau and Ott, we fit the temperature dependence to an expression of the form

$$h_{c2}(T)=h_{c2}(0)[1-(T/T_c)^\mu] \tag{5}$$

for $T \geqslant 90$ K. This describes the data well (solid curve in the lower inset) and yields $\mu=2.5$ and $T_c=134$ K, which is quite close to the diamagnetic onset of 133 K measured in low field. Unfortunately, the scaling analysis provides only relative values for H_{c2}. So it is useful to compare these results with the corresponding determinations of βH_{c2} from the London analysis. This comparison is shown in the upper inset to Fig. 3. The error bars show one standard deviation and the straight line illustrates a simple direct proportionality. While there seems to be a systematic deviation from such a simple relation, most data lie within two standard deviations of a linear dependence.

B. Equilibrium properties of Hg-1223 with randomly oriented CDs

We now address the question of how the addition of randomly oriented columnar defects modifies the equilibrium magnetization in the mixed state. The qualitative effects of the CD's are illustrated in Fig. 1, which includes data for M_{eq} at 77 K for irradiated samples with defect densities $B_\Phi \approx 1.0$ and 3.4 T. Comparing these data with the virgin curve shows that the CD's reduce considerably the magnitude of the equilibrium magnetization, especially at lower fields. In addition, they generate a pronounced deviation from the standard London field dependence, giving M_{eq} an S-like dependence on field. This ''anomalous'' behavior has been observed previously in cuprates containing *parallel* columnar defects formed by 5.8 GeV Pb ions, in thallium-based single crystals;[13] in Bi-2223 tapes;[19] and in Bi-2212 single crystals.[20,21]

These changes in the equilibrium magnetization have been attributed to magnetic interactions between the vortex lattice and the columnar defects. By occupying a pinning site, a vortex gains pinning energy. This reduction in system energy must exceed the energy increase arising from direct intervortex repulsion when a vortex is displaced from its natural position in the lattice to a particular columnar defect. For a defect geometry with parallel tracks that have a Poisson distribution of separations, Wahl *et al.*[13] obtained an expression for M_{eq} that describes reasonably well the S-shaped field dependence in Tl-cuprate crystals containing parallel CD's.

In the Hg-cuprates investigated here, one might expect that the randomly oriented columnar microstructure should entangle the vortices. Consequently, it is somewhat curious that M_{eq} in polycrystalline materials with random CD's can resemble single crystals with parallel defects. The operative ''refocussing'' process is sketched in Fig. 4. (a) In real space, the sample consists of grains randomly oriented with respect to the applied field H. (b) After irradiation, there are CD's randomly oriented about the c axis, which makes some angle θ_H with respect to an applied magnetic field. Now, for highly anisotropic single crystals, it is long recognized that only the normal component of field is effective.[18] More generally, rescaling gives a field $\tilde{H}$ lying near the c axis; similar arguments[10] lead to a refocussing of the CD's into a narrow distribution about the c axis. According to the theoretical development,[10] the complexity of randomly oriented columnar defects in a polycrystalline material is reduced to a considerable degree by a large superconducting anisotropy, restoring the simple physics of a crystal with parallel pins. Indeed, studies of polycrystalline Hg-cuprates demonstrated a recovery of vortex variable range hopping (VRH), very similar to that observed in YBaCuO single crystals containing parallel CD's.[22] Among the Hg cuprates with one, two, and three adjacent Cu-O layers, the recovery of VRH was most pronounced in the Hg-1223 material with the largest mass anisotropy parameter γ. We have suggested[23] that this scenario—an anisotropy-induced refocussing of the defects and field toward the crystalline c axis—can account for the S-like dependence of M_{eq} on field in highly anisotropic Tl-2212 materials, where $\gamma \sim 200$. Here we test and confirm the validity of the rescaling formalism in these Hg-1223 materials with significantly lower $\gamma \sim 60$. Below we show that vortex pinning by random CD's provides a reasonable qualitative explanation for the reduction in equilibrium magnetization, despite the complexity of the materials in real space.

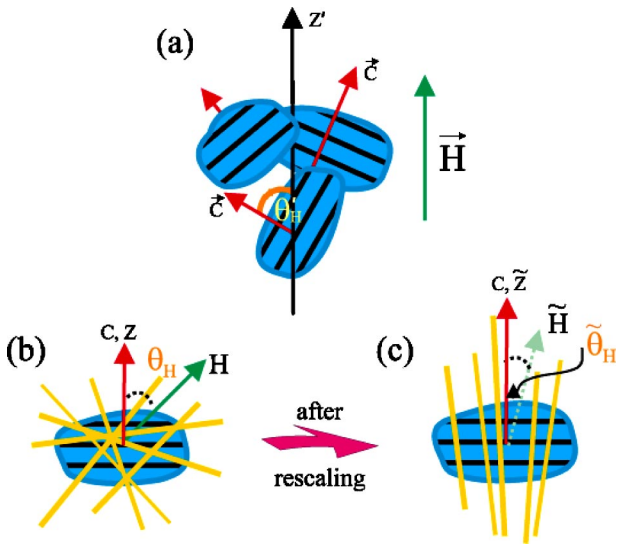

FIG. 4. (Color online) An illustration of the refocussing process. (a) Polycrystalline material with randomly distributed c axes. (b) One grain with randomly oriented columnar defects, in magnetic field with arbitrary orientation θ_H. (c) after rescaling, both the effective field and defect array are tilted close to the c axis (Ref. 10).

Let us now use the vortex-defect interaction theory of Wahl *et al.*[13] to model our experimental data. From the theory, one has for $H \| c$ axis that

$$M_{eq} = -(\varepsilon_0/2\Phi_0)\ln(\beta H_{c2}/B) + \frac{U_0}{\Phi_0}\left\{1 - \left[1 + \frac{U_0 B_\Phi}{\varepsilon_0 B}\right] \times \exp\left(-\frac{U_0 B_\Phi}{\varepsilon_0 B}\right)\right\}, \quad (6)$$

where $\varepsilon_0 = [\Phi_0/4\pi\lambda_{ab}]^2$ is the line energy, $U_0 \propto \varepsilon_0$ is the pinning energy, and $B = (H + 4\pi M) = H$ since M is small. The first term is the conventional London expression. The second is an added term to account for interactions; it is most significant in intermediate fields and it vanishes in large fields $B \gg B_\Phi$, where vortices greatly outnumber defects. For H inclined at angle θ from the c axis, one can introduce the angular dependence of the line energy, pinning energy, and B_{c2} via the anisotropy function Eq. (2). An angular average for a randomly oriented polycrystalline material leads to the following:

$$\langle M_{eq} \rangle = -(\varepsilon_0/2\Phi_0)[(1/2)\ln(\beta H_{c2}/B) + (1/4)] + \frac{U_0}{2\Phi_0}\left\{1 - \left[1 + \frac{U_0 B_\Phi}{\varepsilon_0 B}\right]\exp\left(-\frac{U_0 B_\Phi}{\varepsilon_0 B}\right)\right\}. \quad (7)$$

Here the symbols have the same meaning as above and we assume that $\gamma \gg 1$.

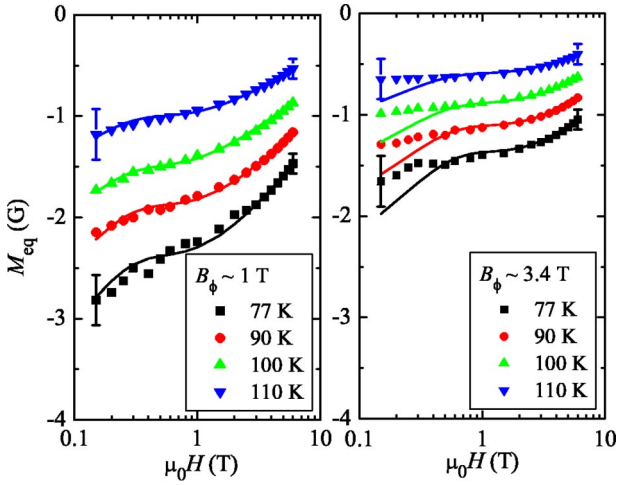

FIG. 5. (Color online) Plots of $M_{eq}(H,T)$ vs ln(H) for irradiated Hg-1223 with (a) $B_\Phi \sim 1$ T and (b) with $B_\Phi \sim 3.4$ T. Symbols are experimental results with estimated error bars, while lines show modeling of data using Eq. (7) where effects of vortex-defect interactions are included.

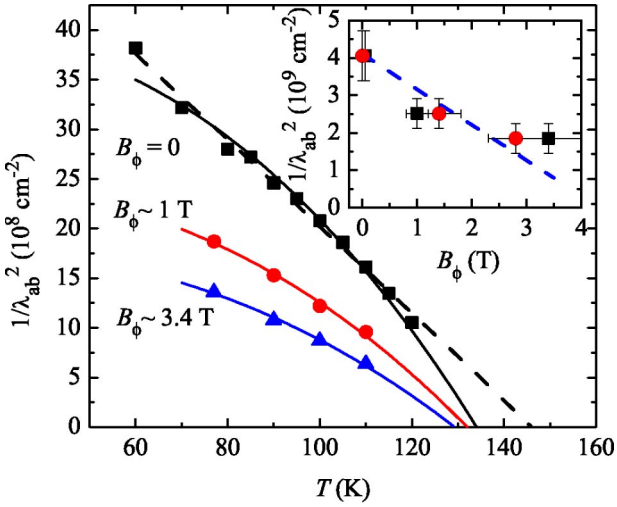

FIG. 6. (Color online) The temperature dependence of the London penetration depth $1/\lambda_{ab}^2$. Values for the virgin sample come from a conventional London analysis of the data in Fig. 5; for the irradiated materials, values come from modeling the equilibrium magnetization shown in Fig. 6. Inset shows values for $1/\lambda_{ab}^2$, extrapolated to $T=0$, plotted vs defect density; square symbols denote B_Φ values calculated from the proton fluence and circular symbols are values used in the modeling.

In using this expression, Eq. (7), to model the data at various temperatures T (77, 90, 100, and 110 K), our objective was to maintain an internally consistent set of parameters. The results are shown as solid lines in Fig. 5(a) for the sample with $B_\Phi \sim 1$ T and in Fig. 5(b) for the sample with a higher defect density. Given the complexity of the polycrystalline material and of the vortex and defect arrays, the description of the experimental data (filled symbols) is relatively good. The values for the pinning energy are a significant fraction of the line energy and are quite reasonable, with $U_0 = 0.8\varepsilon_0$ for both materials. To obtain reasonable modeling of the data for the two irradiated materials, we used values of 1.4 and 2.8 T, respectively, for the effective defect densities B_Φ. The differences from the nominal values (calculated from the proton fluences) may arise from some overlap of tracks at the highest fluence combined with uncertainty in calculating the production rate for CD's. [In analyzing the more highly anisotropic Tl-2212 materials ($\gamma \sim 200$), comparable modeling[23] was achieved with B_Φ values varying by $\sim 20\%$ from those calculated from the proton fluence.] The high density of tracks and their overlap may account in part for the lower quality modeling in Fig. 5(b), where deviations are largest in low fields and where also the averaging procedure described in Sec. II is least valid.

An important feature of any superconducting material is its London penetration depth. Figure 6 summarizes the results for these materials in a plot of $1/\lambda_{ab}^2$ versus temperature. Values for the virgin sample were obtained from a standard London analysis of the data in Fig. 2. An extrapolation of a Ginzburg-Landau linear dependence near T_c (dashed line) to $T=0$ yields a value $\lambda_{ab}(T=0) = 174$ nm, but the implied T_c value is too high. Alternatively, we can invoke the underlying assumption of the scaling procedure[11] that κ is temperature independent, which means that $1/\lambda_{ab}^2$ should have the same temperature dependence as h_{c2}. Hence we fit the present data for the virgin sample ($T \geqslant 90$ K) with the same temperature dependence in Eq. (5) using the same values for T_c and μ and varying only the prefactor $1/\lambda^2(T=0)$, obtaining $\lambda_{ab}(T=0) = 157$ nm, which is comparable with earlier determinations.[24] The resulting fit (solid line in main figure) is "natural," as illustrated by the fact that its extrapolation to lower T lies very near the lower-temperature data.

In Fig. 6, the λ_{ab} values for the materials with CD's were obtained from the modeling procedure. All of these results are reasonably behaved, with $1/\lambda_{ab}^2$ varying roughly linearly with T at high temperature, but extrapolating to T_c values that are rather high. Thus we also fit the data for the irradiated samples with the temperature dependence in Eq. (5), again setting $\mu = 2.5$ and fixing T_c at the experimental values measured in low field, so that only the prefactor $1/\lambda^2(T=0)$ was varied. The resulting fits, which are shown as solid lines in the main figure, describe the data quite well.

It is clear that proton irradiation increased λ_{ab} significantly. This is expected from two theoretical perspectives. First, conventional GLAG (Ginzburg-Landau-Abrikosov-Gorkov) theory[25] predicts that the penetration depth λ^2 increases as $(1+\xi_0/\ell)$ when the electronic mean free path ℓ is reduced by scattering, as produced by irradiation-generated defects from neutrons and secondary protons released by spallation. Second, the theory of Wahl-Buzdin[13] provides that introducing CD's increases the penetration depth as

$$\lambda^{-2}(B_\Phi) = \lambda^{-2}(B_\Phi = 0)[1 - 2\pi R^2 B_\Phi/\Phi_0], \qquad (8)$$

where R is the radius of a columnar track. The combination of these two effects leads to the significant, progressive increases in λ observed in Fig. 6. To compare with Eq. (8), the inset of Fig. 6 shows $1/\lambda_{ab}^2(T=0)$ [the prefactors from fit-

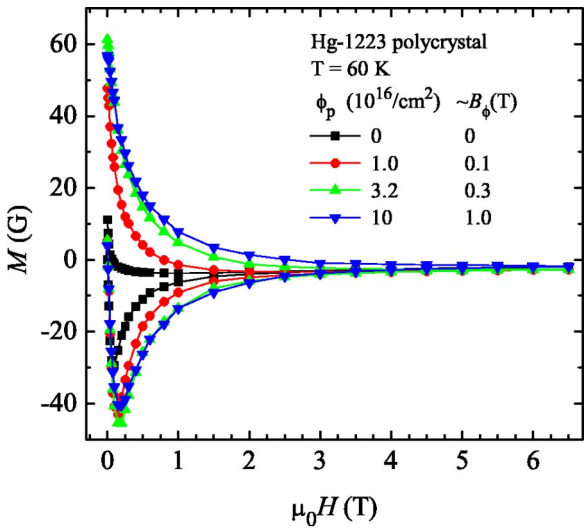

FIG. 7. (Color online) The magnetization of polycrystalline Hg-1223 materials at 60 K vs applied magnetic field. Samples were irradiated with various fluences ϕ_p of 0.8 GeV protons, as shown, to create randomly oriented columnar defects with approximate "matching fields" B_Φ.

ting Eq. (5)] plotted versus defect density. These are plotted as a function of B_Φ values obtained both from the proton fluence (squares) and the modeling procedure (circles), as discussed above. The straight line in the inset illustrates the theoretical dependence in Eq. (8) and agrees qualitatively with the data; the resulting value $R \approx 8.7$ nm is somewhat smaller than the 11 nm value obtained for Tl-2212 materials.[23] In each case, it is likely that the CD's have a large effective radius due to oblique passage of ions through CuO planes and an oxygen-depleted region surrounding the amorphous track.[26]

An interesting consequence of a larger London penetration depth is that the vortex line energy $\varepsilon_0 \sim 1/\lambda_{ab}^2$ decreases significantly. As a result, one can expect the vortex pinning energy of a CD and its pinning force to decrease, reducing its effectiveness. A progressive decrease of ε_0 can be expected to counteract the nominally positive influence of increasing the defect density B_Φ. Consequently it is interesting and useful to examine how the irreversible properties of the materials change with defect density, which we now consider.

C. Irreversible properties and persistent current density

As is well recognized, the addition of correlated disorder can increase the pinning of vortices, often quite significantly. This is illustrated in Fig. 7, which shows the magnetization $M(H)$ at 60 K versus magnetizing field H, for various defect densities. With increasing fluence, the "hysteresis loops" increase in width and become symmetric about the $M=0$ axis.

For the virgin sample, the asymmetry, in combination with the fact that the decreasing field branch lies near the $M=0$ axis, suggests that surface barriers[27–29] contribute to the observed hysteresis in this case. It is interesting to note that a relatively low dosage of CD's, $B_\Phi = 0.1$ T, symmetrizes the $M(H)$ loop significantly; in particular, the magnitude of M in the decreasing field branch is much larger. These features imply that the addition of CD's suppresses the surface barrier, as recently discussed by Koshelev and Vinokur.[30]

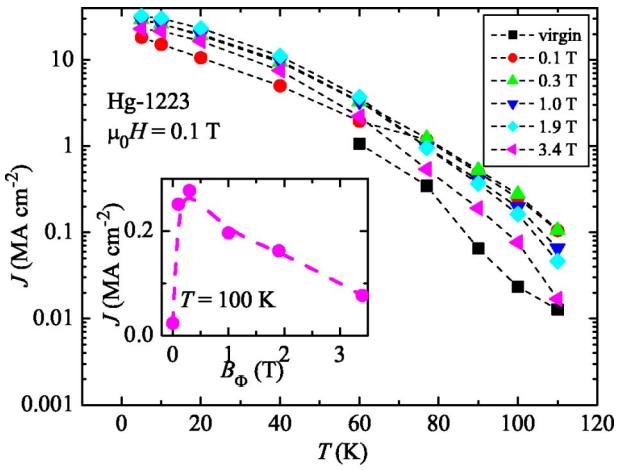

FIG. 8. (Color online) The intragranular persistent current density J vs temperature for various irradiated materials, measured in applied magnetic field of 0.1 T. The inset shows that J at 100 K is maximized at a defect density of 0.1–0.3 T.

Using the Bean model, one may obtain the persistent current density $J(H,T)$. For these porous materials with randomly oriented, high-angle grain boundaries that are weakly linked, the magnetization reflects the *intragranular* current density. Some results of this analysis are shown in Figs. 8 and 9 as plots of J versus temperature T, in applied fields of 0.1 and 1 T, respectively. The enhancement in J is modest in low fields; this can be attributed to the presence in the virgin sample of both naturally occurring defects that provide some pinning and the likely influence of surface barrier effects, as already noted. In higher fields, the contribution of the random CD's is more apparent and J is enhanced by about an order of magnitude. For high-T_c materials with these angularly dispersed defects, one generally achieves the maximum

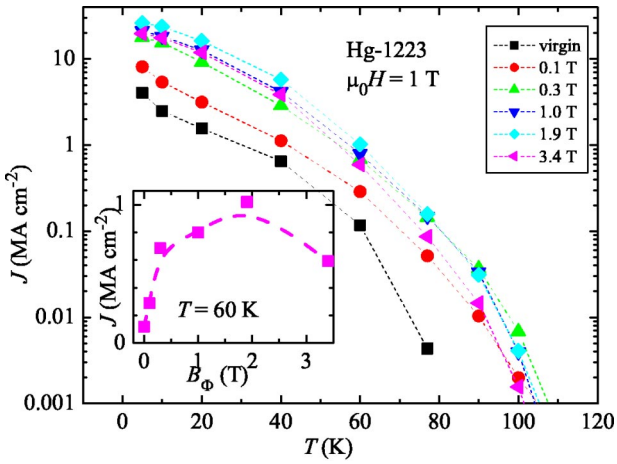

FIG. 9. (Color online) The intragranular persistent current density J vs temperature for various irradiated materials, measured in applied magnetic field of 1 T. Inset: J at 60 K vs defect density B_Φ exhibits a maximum at a defect density of ~2 T.

J at some defect density B_Φ near 0.2–2 T. This optimization is shown by the insets in Figs. 8 and 9. For an applied field of 0.1 T (Fig. 8 inset), J at 100 K is largest for $B_\Phi = 0.1$–0.3 T. For the second example with a field of 1 T (Fig. 9 inset), J at 60 K is largest for B_Φ near 2 T. Qualitatively, the optimum defect density in each case is comparable with the vortex density, i.e., about 2 times larger.

For higher defect densities, the current density J decreases. This is due primarily to a suppression of the vortex line energy and pinning energy, as a consequence of the large, experimentally observed increases in the London penetration depth. Thus we believe that *the competition between increasing defect density and weakening line energy plays a major role in determining the range of B_Φ that maximizes the current density J*, as illustrated in the insets of Figs. 8 and 9. This competition is reminiscent of the formation of point-like defects in $YBa_2Cu_3O_{7-\delta}$, where progressive removal of oxygen creates defects, but also reduces their effectiveness through increases in the superconductive length scales.[31,32]

An additional mechanism for reducing J at higher defect densities may be that the presence of additional CD's helps us to initiate the hopping of vortices to nearby empty pinning sites. A third potential influence is a suppression of T_c; however, the change in T_c is small and these measurements are far from T_c, so this contribution is expected to be small.

IV. SUMMARY

We irradiated polycrystalline $HgBa_2Ca_2Cu_3O_x$ materials with 0.8 GeV protons to produce randomly oriented columnar defects via a fission process. Adding random linear defects significantly reduced the magnitude of the equilibrium magnetization M_{eq} and changed its dependence on magnetic field from a simple London ln(H) form (as observed for the virgin material) to a more complex S-shaped dependence. For the virgin superconductor, $M_{eq}(H,T)$ can be scaled by the relative upper critical field $h_{c2}(T)$, as recently discussed;[12] these results compare reasonably with values from a London analysis. For materials with random CD's, we invoke an anisotropy-induced refocusing of the vortex-defect array and model these results using the theory of Wahl-Buzdin that incorporates vortex-defect interactions. This analysis shows that the addition of random columnar defects increases the London penetration depth markedly. The success of this analysis demonstrates the essential correctness and applicability of the refocussing mechanism in these materials with intermediate anisotropy $\gamma \sim 60$. Enhancements in vortex pinning increased the persistent current density J, with the optimum defect density depending on the range of field and temperature. However, a high density of CD's increases λ and decreases the line energy, which diminishes their effectiveness for pinning vortices. Finally, the study provides qualitative evidence for the suppression of surface barriers in these Hg-1223 materials by a low density of CD's. Overall, we find a delicate balance between increases in the density of correlated disorder—randomly oriented columnar defects—and decreases in the equilibrium superconductive properties, which progressively reduce the effectiveness of each defect added.

ACKNOWLEDGMENTS

We thank M. Paranthaman for providing the starting Hg-1223 materials used in this study, and thank I. L. Landau for communicating their results prior to publication. The work of J.G.O. was supported in part by the Chilean FONDECYT, Grant No. 1000394. Oak Ridge National Laboratory is managed by UT-Battelle, LLC for the U.S. Department of Energy under Contract No. DE-AC05-00OR22725. Los Alamos National Laboratory is funded by the U.S. Department of Energy under Contract No. W-7405-ENG-36.

*Present address: Department of Physics and Astronomy, Michigan State University, East Lansing, Michigan.

†Present address: Korea Electrotechnology Research Institute, Changwon, Kyung-Nam, 641-120 Korea.

‡Present address: Department of Physics, University of Nebraska, Lincoln, Nebraska.

[1] L. Civale, T.K. Worthington, L. Krusin-Elbaum, A.D. Marwick, F. Holtzberg, J.R. Thompson, M.A. Kirk, and R. Wheeler, JOM **44**, 60 (1992).

[2] D.R. Nelson and V.M. Vinokur, Phys. Rev. B **48**, 13 060 (1993).

[3] T. Hwa, P. Le Doussal, D.R. Nelson, and V.M. Vinokur, Phys. Rev. Lett. **71**, 3545 (1993).

[4] G. Blatter, M.V. Feigel'man, V.B. Geshkenbein, A.I. Larkin, and V.M. Vinokur, Rev. Mod. Phys. **66**, 1125 (1994).

[5] L. Krusin-Elbaum, J.R. Thompson, R. Wheeler, A.D. Marwick, C. Li, S. Patel, D.T. Shaw, P. Lisowski, and J. Ullmann, Appl. Phys. Lett. **64**, 3331 (1994).

[6] H. Safar, J.H. Cho, S. Fleshler, M.P. Maley, J.O. Willis, J.Y. Coulter, J.L. Ullmann, P.W. Lisowski, G.N. Riley, M.W. Rupich, J.R. Thompson, and L. Krusin-Elbaum, Appl. Phys. Lett. **67**, 130 (1995).

[7] J.R. Thompson, L. Krusin-Elbaum, D.K. Christen, K.J. Song, M. Paranthaman, J.L.Ullmann, J.Z. Wu, Z.F. Ren, J.H. Wang, J.E. Tkaczyk, and J.A. DeLuca, Appl. Phys. Lett. **71**, 536 (1997).

[8] C. Klein, H.W. Weber, B. Moss, R. Zeng, S.X. Dou, R. Sawh, Y. Ren, and R. Weinstein, Appl. Phys. Lett. **73**, 3935 (1998), and references therein.

[9] J.R. Thompson, J.G. Ossandon, L. Krusin-Elbaum, K.J. Song, D.K. Christen, and J.L. Ullmann, Appl. Phys. Lett. **74**, 3699 (1999).

[10] L. Krusin-Elbaum, G. Blatter, J.R. Thompson, D.K. Petrov, R. Wheeler, J. Ullmann, and C.W. Chu, Phys. Rev. Lett. **81**, 3948 (1998).

[11] I.L. Landau and H.R. Ott, Phys. Rev. B **66**, 144506 (2002).

[12] I.L. Landau and H.R. Ott, Physica C **385**, 544 (2003).

[13] A. Wahl, V. Hardy, J. Provost, C. Simon, and A. Buzdin, Physica C **250**, 163 (1995).

[14] M. Paranthaman, Physica C **222**, 7 (1994).

[15] L. Krusin-Elbaum, D. Lopez, J.R. Thompson, R. Wheeler, J. Ullmann, C.W. Chu, and Q.M. Lin, Nature (London) **250**, 243 (1997).

[16] Z. Hao, J.R. Clem, M.W. McElfresh, L. Civale, A.P. Malozemoff,

and F. Holtzberg, Phys. Rev. B **43**, 2844 (1991).
[17] V.G. Kogan, M.M. Fang, and Sreeparna Mitra, Phys. Rev. B **38**, 11 958 (1988).
[18] G. Blatter, V.B. Geshkenbein, and A.I. Larkin, Phys. Rev. Lett. **68**, 875 (1992).
[19] Q. Li, Y. Fukumoto, Y. Zhu, M. Suenaga, T. Kaneko, K. Sato, and C. Simon, Phys. Rev. B **54**, R788 (1996).
[20] C.J. van der Beek, M. Konczykowski, T.W. Li, P.H. Kes, and W. Benoit, Phys. Rev. B **54**, R792 (1996).
[21] C.J. van der Beek, M. Konczykowski, R.J. Drost, P.H. Kes, N. Chikumoto, and S. Bouffard, Phys. Rev. B **61**, 4259 (2002), and references therein.
[22] J.R. Thompson, L. Krusin-Elbaum, L. Civale, G. Blatter, and C. Feild, Phys. Rev. Lett. **78**, 3181 (1997).
[23] J.G. Ossandon, J.R. Thompson, L. Krusin-Elbaum, H.J. Kim, D.K. Christen, K.J. Song, and J.L. Ullmann, Supercond. Sci. Technol. **14**, 666 (2001).
[24] J. R. Thompson, in *Studies of High Temperature Superconductors*, edited by A.V. Narlikar (Nova Science, Commack, NY, 1998), Vol. 26, pp. 113–131.
[25] T.P. Orlando, E.J. McNiff, Jr., S. Foner, and M.R. Beasley, Phys. Rev. B **19**, 4545 (1979).
[26] Y. Zhu, Z.X. Cai, R.C. Budhani, M. Suenaga, and D.O. Welch, Phys. Rev. B **48**, 6436 (1993).
[27] Y.R. Sun, J.R. Thompson, H.R. Kerchner, D.K. Christen, M. Paranthaman, and J. Brynestad, Phys. Rev. B **50**, 3330 (1994).
[28] J.A. Lewis, V.M. Vinokur, J. Wagner, and D. Hinks, Phys. Rev. B **52**, R3852 (1995).
[29] Y.C. Kim, J.R. Thompson, D.K. Christen, Y.R. Sun, M. Paranthaman, and E.D. Specht, Phys. Rev. B **52**, 4438 (1995).
[30] A.E. Koshelev and V.M. Vinokur, Phys. Rev. B **64**, 134518 (2001).
[31] J.G. Ossandon, J.R. Thompson, D.K. Christen, B.C. Sales, H.R. Kerchner, J.O. Thomson, Y.R. Sun, K.W. Lay, and J.E. Tkaczyk, Phys. Rev. B **45**, 12 534 (1992).
[32] J.G. Ossandon, J.R. Thompson, D.K. Christen, B.C. Sales, Y.R. Sun, and K.W. Lay, Phys. Rev. B **46**, 3050 (1992).